PROCEEDINGS, 51st Workshop on Geothermal Reservoir Engineering
Stanford University, Stanford, California, February 9-11, 2026
SGP-TR-230

Mitigating Post-injection Induced Seismicity in Enhanced Geothermal Systems (EGS): The Role of Pressure-dependent Hydraulic Diffusivity in Stimulated Fractures

Yuan Tian, Roland Horne

Department of Energy Science and Engineering, Stanford University, California 94305, United States

ytian96@stanford.edu

Keywords: induced seismicity, hydraulic fractures, hydro-mechanical effect, EGS

ABSTRACT

Delayed induced seismicity remains one of the major challenges for Enhanced Geothermal Systems (EGS), particularly when large earthquakes occur weeks to months after prolonged mitigation efforts. At the Pohang EGS site, a Mw 5.5 earthquake occurred approximately two months after injection stopped, following extended post-injection flowback that recovered less than half of the injected fluid. Although fluid-pressure diffusion has been identified as a dominant mechanism driving this delayed earthquake, the physical reasons why flowback failed to sufficiently depressurize the reservoir remain unclear. Motivated by field observations showing strongly pressure-dependent and largely reversible hydraulic diffusivity within the stimulated fracture zone around the injection well, we investigated the role of pressure-sensitive stimulated fractures in post-injection mitigation failure. We developed a pressure-diffusion model that explicitly incorporates pressure-dependent hydraulic diffusivity and evaluated post-injection pressure evolution under different mitigation strategies. Our results show that rapid flowback in unpropped fractures, as implemented at Pohang, can be ineffective despite generating large reverse pressure gradients toward the well. Rapid depressurization near the well induces fracture closure and a sharp collapse in near-well permeability, transforming stimulated fractures from high-transmissivity conduits into hydraulic barriers. As a result, excess pressure remains trapped away from the well and continues to diffuse toward the fault, producing substantial delayed fault pressurization consistent with the timing of the Mw 5.5 event. Modifying well operation strategies by adjusting the rate of wellhead pressure depressurization alone provides only limited improvement. In contrast, preserving fracture diffusivity through addition of proppant substantially enhances pressure reduction and slows fault pressurization, with rapid flowback combined with proppant providing the most effective mitigation tested in this study. These findings highlight the importance of fracture hydromechanical behavior in post-injection seismic risk mitigation.

1. INTRODUCTION

Enhanced Geothermal Systems (EGS) offer a promising pathway toward sustainable, low-carbon energy by enabling heat extraction from high-temperature, low-permeability reservoirs through hydraulic stimulation (Horne et al., 2025). Despite this potential, EGS development has been repeatedly challenged by induced seismicity, particularly large events occurring during the post-injection period (Ellsworth et al., 2019; Woo et al., 2019; Boyet 2023; Boyet et al., 2024b; Kivi et al., 2023, 2025). In several projects, seismicity has not stopped following injection termination but instead intensified hours to months later, in some cases culminating in damaging earthquakes. Notable examples include the Mw 5.5 Pohang earthquake, which occurred approximately two months after injection stopped (Ellsworth et al., 2019; Woo et al., 2019), and the Basel EGS project, where the largest Mw 2.9 event occurred five hours after shut-in (Häring et al., 2008; Deichmann et al., 2009). These delayed post-injection earthquakes have led to temporary or permanent suspension of geothermal projects, underscoring the urgent need for effective mitigation strategies (Boyet et al., 2024a; Tangirala et al., 2024) that can reduce seismic hazard during the post-injection phase.

In practice, injection-stage seismicity is commonly used as an operational indicator to activate mitigation actions intended to prevent large post-injection events. Common mitigation strategies include shut-in, in which the well is closed and neither injection nor extraction occurs, and flowback (or bleed-off), in which the well is opened to reduce wellhead pressure and promote fluid withdrawal from the reservoir. Shut-in was applied in the Basel project (Häring et al., 2008; Deichmann et al., 2009), while flowback was implemented at Pohang (Ellsworth et al., 2019; Min et al., 2023). However, these strategies have not always been effective in preventing large, delayed events. At Pohang, the onset of flowback was followed by a prolonged quiescent period of approximately 57 days, after which seismicity resumed abruptly and culminated in the Mw 5.5 earthquake. Moreover, despite nearly two months of flowback, less than half of the injected fluid volume was recovered (Ellsworth et al., 2019; Woo et al., 2019; Min et al., 2023). The limited effectiveness of current mitigation efforts motivates a closer examination of the physical processes and key controlling factors governing delayed post-injection seismicity.

Post-injection earthquakes in Enhanced Geothermal Systems can arise from multiple physical mechanisms (Ellsworth et al., 2013; Moein et al., 2023), including direct pore-pressure effects (Ellsworth et al. 2013), poroelastic stress changes associated with pressure diffusion in the rock matrix (Chang et al., 2020; Yeo et al., 2020; Lim et al., 2020), and elastic stress transfer from earthquake interactions (Catalli et al., 2013). The relative importance of these mechanisms may vary among projects depending on in-situ geological conditions and operations. Among these mechanisms, fluid-pressure diffusion has been widely identified as a key process contributing to the delayed post-injection seismicity following injection termination. During the post-injection period, elevated pressure near the well can persist and migrate outward through the reservoir toward nearby faults. When pressure propagates beyond the stimulated fracture zone into low-diffusivity basement formations, diffusion can be sufficiently slow to produce delays of days to months between injection cessation and fault pressurization. Once the pressure front reaches a nearby fault, pressure buildup reduces effective normal stress and may trigger fault

activation, resulting in delayed earthquakes. Owing to the finite speed of pressure diffusion and the resulting temporal separation between injection termination and fault pressurization, fluid pressure is therefore widely regarded as a primary mechanism governing delayed induced seismicity and is the focus of the present study.

Motivated by the key role of pressure diffusion, existing studies have investigated delayed induced seismicity by modeling fault pressurization driven by pressure diffusion between the injection well and the post-injection earthquake hypocenter (Ellsworth et al., 2019; Chang et al., 2020; Yeo et al., 2020; Lim et al., 2020; Kim et al., 2023; Alcolea et al., 2024). In most existing models, the temporal evolution of fluid pressure on faults is evaluated by prescribing hydraulic diffusivity along the flow path from the well to the fault, with diffusivity at a given location commonly treated as constant in time during both injection and post-injection periods. Such models have been successful in reproducing delayed pressure arrival at distant faults and capturing the timing of post-injection seismicity. However, these approaches generally do not examine how reservoir pressurization during injection and depressurization during post-injection operations may be influenced by temporal variations in hydraulic properties. Besides, the physical reasons why early-activated and prolonged mitigation efforts, such as the approximately two-month flowback at the Pohang EGS site, resulted in limited fluid recovery and ultimately failed to sufficiently depressurize the reservoir and results in delayed large earthquake have rarely been investigated explicitly.

A potential factor not represented in constant-diffusivity models is the pressure-dependent hydraulic behavior of fractures, particularly for the near-well stimulated fracture zone in Enhanced Geothermal Systems (EGS). Theoretical models, laboratory experiments and field observations demonstrate coupled hydromechanical behavior of fractures in which fluid pressure acting within fractures reduces effective normal stress and induces fracture mechanical deformation as fracture aperture changes. Because fracture aperture directly controls the effective flow-channel size, this deformation strongly influences fracture hydraulic properties including permeability and hydraulic diffusivity commonly described by the cubic law (Witherspoon, 1980). This pressure-dependent hydraulic behavior has also been observed in stimulated fractures in EGS. At Pohang, in-situ measurements from the stimulated fracture zone surrounding the hydraulic-fracture–dominated well whose stimulation is directly linked to activation of the delayed Mw 5.5 earthquake show that hydraulic diffusivity within the stimulated hydraulic fractures is strongly pressure-dependent, varying by up to three orders of magnitude with largely reversible changes during pressurization and depressurization (Park et al., 2017; Park et al., 2020). These observations indicate that fracture hydraulic diffusivity evolves dynamically during injection and post-injection operations rather than remaining constant. Pressure-dependent fracture diffusivity has important consequences for pressure diffusion. Semi-analytical solutions that incorporate pressure-dependent permeability or diffusivity show that, during injection, fracture opening under elevated fluid pressure produces nonlinear diffusion characterized by relatively flat pressure profiles near the injection point and steeper gradients near the pressure front (Murphy et al., 2004) away from the injection point. Conversely, during depressurization as mitigation during flowback, rapid pressure reduction near the well promotes fracture closure, sharply reducing near-well diffusivity and limiting fluid transmission from more distant regions, thereby trapping elevated pressure away from the well (Zheng, 2025 a, b). The strong and largely reversible pressure dependence of fracture hydraulic properties suggests that such hydro-mechanical coupling can strongly influence post-injection pressure evolution and, consequently, mitigation effectiveness.

Motivated by these observations, we hypothesize that strongly pressure-dependent hydraulic diffusivity in stimulated fractures could be a key factor contributing to flowback ineffectiveness during post-injection mitigation. When flowback rapidly reduces wellhead pressure, the resulting pressure drop in near-well stimulated fractures promotes closure and a sharp decrease in diffusivity. Stimulated fractures may thus transition from effective high-transmissivity conduits to hydraulic barriers, hindering sustained fluid extraction and limiting pressure reduction beyond the near-well stimulated region. Near-well diffusivity collapse during flowback can lead to incomplete reservoir depressurization and the development of trapped high pressure away from the well. Although pressure diffusion toward distant faults may be slow due to low basement diffusivity, the magnitude of trapped reservoir pressure can still drive rapid and large fault pressurization once the pressure front arrives, potentially exceeding activation thresholds and triggering delayed seismicity after a prolonged quiescent period. Thus, in systems with strongly pressure-dependent fracture diffusivity, post-injection seismicity may be delayed but not necessarily prevented by conventional flowback. Recognizing the role of pressure-dependent fracture hydraulic behavior, we examined mitigation strategies aimed at enhancing post-injection pressure reduction in the reservoir and on nearby faults. One approach is well operation strategies by adjusting the rate of wellhead pressure reduction to limit fracture closure and maintain higher diffusivity during flowback. We evaluated three representative strategies: shut-in, rapid flowback, and gradual flowback. Beyond the well operational control, we explored mitigation by modifying fracture properties to weaken the coupling between diffusivity and pressure during depressurization. Proppants as stiff granular materials increasingly used in EGS projects such as Utah FORGE and Fervo, mechanically support fracture apertures under decreasing pressure. By maintaining transmissivity during flowback, proppant-supported fractures can sustain higher diffusivity, enabling more effective pressure reduction and fluid extraction than strategies relying solely on well operation.

This study identified strongly pressure-dependent hydraulic diffusivity in stimulated fractures as a key factor limiting the effectiveness of flowback-based mitigation in EGS. Using numerical modeling, we assessed post-injection mitigation strategies for reducing trapped reservoir pressure and slowing fault pressurization, comparing shut-in, rapid flowback, and gradual flowback scenarios with and without proppant-supported fractures. We found that operational adjustments alone provide limited improvement when diffusivity is strongly pressure-dependent, whereas maintaining fracture transmissivity with proppants substantially enhances mitigation. In our model, the combination of proppant-supported fractures and rapid flowback yielded the most effective reservoir depressurization and the slowest fault pressure buildup.

2. FIELD OBSERVAITONS AT THE EGS PROJECT, POHANG, SOUTH KOREA

The Pohang Enhanced Geothermal System (EGS) project, initiated in 2011, was the first EGS development in South Korea and aimed to establish a hydraulic connection between two deep wells (PX-1 and PX-2) for geothermal heat extraction (Ellsworth et al., 2019; Woo et

al., 2019; Min et al., 2023). During the stimulation phase, however, a damaging Mw 5.5 earthquake occurred in November 2017, leading to the permanent shutdown of the project. Seismic observations indicate that stimulation of the hydraulic-fracture–dominated PX-2 well activated a previously unidentified nearby fault, which ultimately hosted the Mw 5.5 event (Ellsworth et al., 2019; Woo et al., 2019). Because this study focuses on the delayed Mw 5.5 earthquake and the failure of post-injection mitigation, we concentrate here on observations associated with the PX-2 well and the reactivated fault; accordingly, figures in this section show only the PX-2 well and the associated seismicity. Importantly, the Mw 5.5 earthquake occurred nearly two months after injection had ceased, classifying it as a post-injection seismic event. During stimulation of the PX-2 well, seismicity increased progressively and reached moderate magnitudes up to Mw 1.67, prompting the activation of a flowback (bleed-off) mitigation strategy. The well was opened to reduce wellhead pressure and withdraw injected fluid, with the goal of depressurizing the reservoir and mitigating the risk of larger events. Despite approximately two months of flowback operations, this mitigation effort failed to prevent the delayed Mw 5.5 earthquake.

The PX-2 well was drilled to a depth of approximately 4.2 km and hydraulically stimulated in three stages, with the third and final stimulation conducted in September 2017 (Figure 1). Stimulation of PX-2 activated a large fault that had not been identified prior to the project and later hosted the delayed Mw 5.5 earthquake. The hypocenter of the mainshock was located approximately 560 m from the PX-2 well (Woo et al., 2019). At the PX-2 depth, the in-situ stress regime was characterized as reverse faulting, with the minimum principal stress (S_3) oriented vertically and estimated at approximately 68 MPa. During stimulation, the maximum wellhead pressure reached about 90 MPa, exceeding S_3 by roughly 22 MPa, indicating the initiation and propagation of hydraulic fractures in the vicinity of the well (Min et al., 2023). Figure 1(left) shows the spatial distribution of seismic events associated with the activated fault relative to the PX-2 well, while Figure 1(right) presents the temporal evolution of seismic event magnitudes together with the cumulative net injection volume. The third stimulation began on 12 September 2017 and lasted approximately 17 days (Stage I). During this period, seismicity increased progressively in both rate and magnitude, reaching a maximum observed magnitude of Mw 1.67 near the end of injection. In response, a flowback (bleed-off) mitigation strategy was initiated immediately after injection ceased. The well was opened to rapidly reduce wellhead pressure and establish a reverse pressure gradient intended to withdraw fluid and depressurize the reservoir. Following the onset of flowback, seismicity declined rapidly and the system entered a quiescent period with no detected events lasting approximately 57 days (Stage II). This quiescence was abruptly terminated by renewed seismicity (Stage III), culminating in the Mw 5.5 earthquake on 15 November 2017. Despite nearly two months of flowback operations, only about 48% of the injected fluid volume was recovered, suggesting that a substantial fraction of the injected fluid remained trapped within the reservoir (Woo et al., 2019; Min et al., 2023).

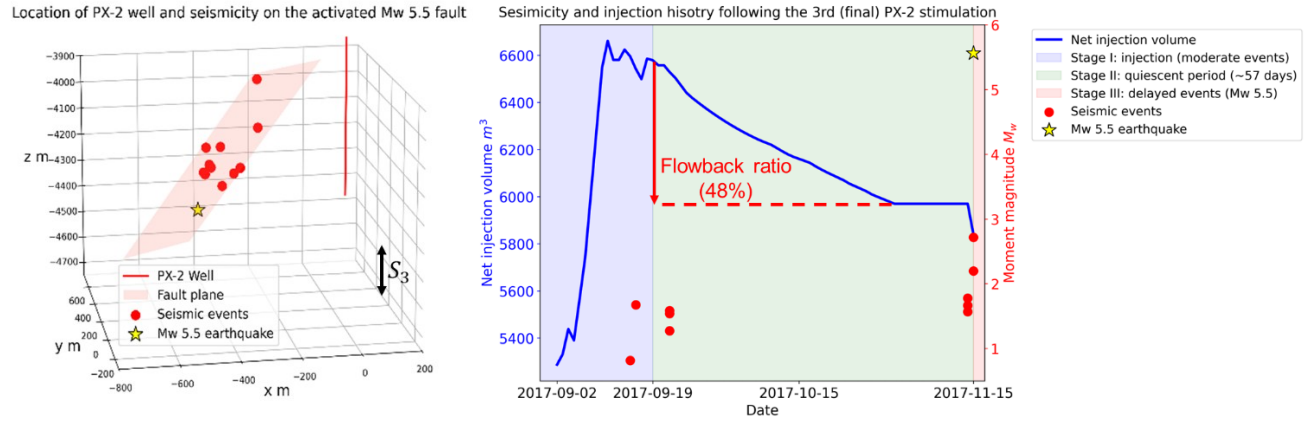

Figure 1: Seismicity and injection history associated with the third (final) stimulation of the PX-2 well at the Pohang EGS site. Spatial distribution of seismic events (left) and temporal evolution of seismic event magnitudes together with the cumulative net injection volume (right).

In-situ injectivity tests conducted at the PX-2 well provide key constraints on the hydraulic behavior of the stimulated fracture zone (Park et al., 2017; Park et al., 2020) in Figure 2. These tests showed that hydraulic properties within the stimulated fractures are strongly pressure-dependent (Figure 2). During pressurization in the injection period, elevated fluid pressure promoted fracture opening, leading to a substantial enhancement of hydraulic diffusivity by up to three orders of magnitude from background basement values of approximately 10^{-3} m² s^{-1} to values approaching 10 m² s^{-1} within the stimulated zone. During depressurization following injection termination, pressure reduction caused fracture closure and a corresponding decrease in hydraulic diffusivity. Importantly, these changes were observed to be largely reversible (Park et al., 2017; Park et al., 2020). These field observations demonstrate that hydraulic diffusivity within the stimulated fracture zone around PX-2 evolved dynamically during both injection and post-injection operations, providing a critical physical basis for the hypothesis that pressure-sensitive stimulated fractures can limit flowback efficiency and contribute to delayed seismicity.

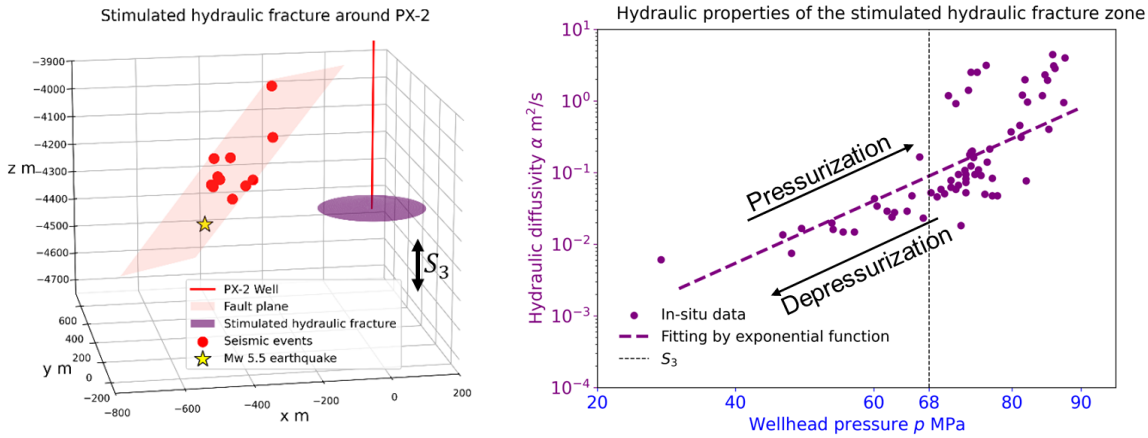

Figure 2: Pressure-dependent hydraulic properties of the stimulated fracture zone around the PX-2 well. Conceptual representation of the stimulated hydraulic fracture (left) and inferred fracture hydraulic diffusivity as a function of pressure (right) from in-situ test (replotted from Park et al., 2017; Park et al., 2020).

3. CONCEPTUAL MODEL

3.1 Physical understanding: Pressure-sensitive stimulated fractures as a cause of flowback failure and delayed seismicity

Field observations at the Pohang EGS site show that a delayed large seismic event as the Mw 5.5 earthquake occurred despite early activation of a flowback mitigation strategy and a prolonged post-injection quiescent period (Section 2). Previous studies have consistently identified fluid-pressure diffusion as the dominant mechanism controlling this delayed earthquake (Ellsworth et al., 2019; Lim et al., 2019; Yeo et al., 2019; Chang et al., 2020). After injection stopped and flowback mitigation strategy was activated, pressure continued to diffuse toward the fault and reached the fault over a timescale of weeks up to months, eventually pressurizing the fault and triggering delayed seismicity. However, an important question that has not been fully investigated is why flowback, which intended to withdraw injected fluid and reduce reservoir pressure, recovered only a limited fraction of the injected volume during the ~57-day flowback period. Addressing this question is important because ineffective flowback implies ineffective pressure reduction in the reservoir, which directly controls the speed and magnitude of delayed fault pressurization and consequently the seismic hazard risk in post-injection period. Motivated by field observations of strongly pressure-dependent and reversible hydraulic diffusivity in the stimulated fracture zone at PX-2 (Section 2), we hypothesize that pressure-sensitive stimulated fractures play a key role in limiting flowback efficiency and reservoir depressurization. Figure 3 illustrates the conceptual model underlying this hypothesis.

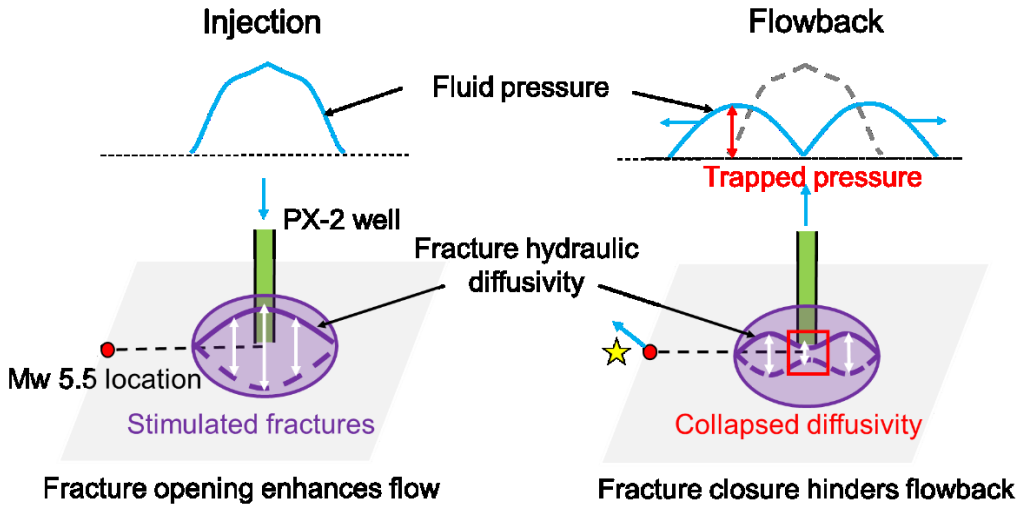

Figure 3: Conceptual illustration of pressure-sensitive stimulated fractures as a mechanism for flowback failure and delayed seismicity.

During high-pressure injection (Figure 3, left), fluid pressure near the well is elevated and can exceed the minimum principal stress, promoting opening of stimulated fractures and substantially enhancing hydraulic diffusivity in the near-well stimulated fracture. Under these conditions, the stimulated fractures act as high-diffusivity pathways that facilitate pressure diffusion away from the well toward the nearby fault. By the end of injection, the pressure front is still propagating toward the fault but has not yet reached it.

After injection stops and the flowback mitigation strategy started (Figure 3, right), the well is opened, which rapidly reduces wellhead pressure and establishing a reverse pressure gradient directed toward the well. In principle, this reverse gradient should promote fluid withdrawal from the well and reservoir depressurization. However, the abrupt pressure reduction near the well also removes pressure support within the stimulated fractures and causes fracture closure. As a result, hydraulic diffusivity in the fracture collapses sharply, causing the fractures transit from high-diffusivity conduits into a low-diffusivity zone acting as a hydraulic barrier. This diffusivity collapse hinders sustained flowback from regions away the well, and leads to trapped pressure with high magnitude in the reservoir. Once pressure front arrives the fault, driven by the high trapped pressure, pressure buildup on fault can be rapid and can exceed the fault activation threshold, triggering delayed seismicity despite the extended period of quiescence during flowback.

3.2 Governing equation and model formulation

To test the hypothesis proposed in Section 3.1, we developed a numerical pressure-diffusion model that explicitly incorporates pressure-dependent hydraulic diffusivity in stimulated fractures. The model is designed to evaluate how pressure-sensitive fracture behavior influences post-injection pressure reduction and the subsequent evolution of fault pressurization under different mitigation strategies.

3.2.1 Governing equation: fluid pressure diffusion with pressure-dependent hydraulic diffusivity

Fluid-pressure evolution along the hydraulic pathway between the PX-2 well and the Mw 5.5 hypocenter (Figure 4) is modeled using a two-dimensional pressure-diffusion equation in Equation (1):

$$\frac{\partial p}{\partial t} - \frac{\partial\left(\alpha\frac{\partial p}{\partial x}\right)}{\partial x} - \frac{\partial\left(\alpha\frac{\partial p}{\partial y}\right)}{\partial y} = \bar{s} \tag{1}$$

where p is fluid pressure, $\alpha(p)$ is the hydraulic diffusivity which is pressure-dependent in the stimulated fracture zone around the well, $\bar{s}$ is the source/sink term divided by total compressibility and porosity.

The PX-2 well is located at the center of the model domain located at $\boldsymbol{x}_{well} = (x_{well}, y_{well}) = (0, 0)$ (Figure 4, left). The model consists of two hydraulic zones in Figure 4: (1) a stimulated hydraulic fracture zone near the well where fluid pressure exceeded the minimum principal stress S_3 during injection and hydraulic fractures opened, and hydraulic diffusivity is strongly pressure-dependent; and (2) an unstimulated basement zone characterized by low and pressure-independent hydraulic diffusivity in basement rock. The spatial extent of the stimulated zone is defined by the region in which fluid pressure exceeded the minimum principal stress (S_3 =68 MPa) at the end of injection. Although pressure diffusion beyond this zone is inherently three-dimensional, we adopted a two-dimensional approximation to provide a conservative upper-bound estimate of pressure at the Mw 5.5 hypocenter location which is ~560 m from the PX-2 well. The diffusion equation is solved using a finite-volume scheme with implicit time stepping on a 2000 m × 2000 m domain discretized into 101 × 101 elements. No-flow boundary conditions are applied on all four sides to ensure that pressure fronts do not reach the model boundaries before the time of the delayed Mw 5.5 earthquake, thereby minimizing boundary effects on fault-pressure estimates.

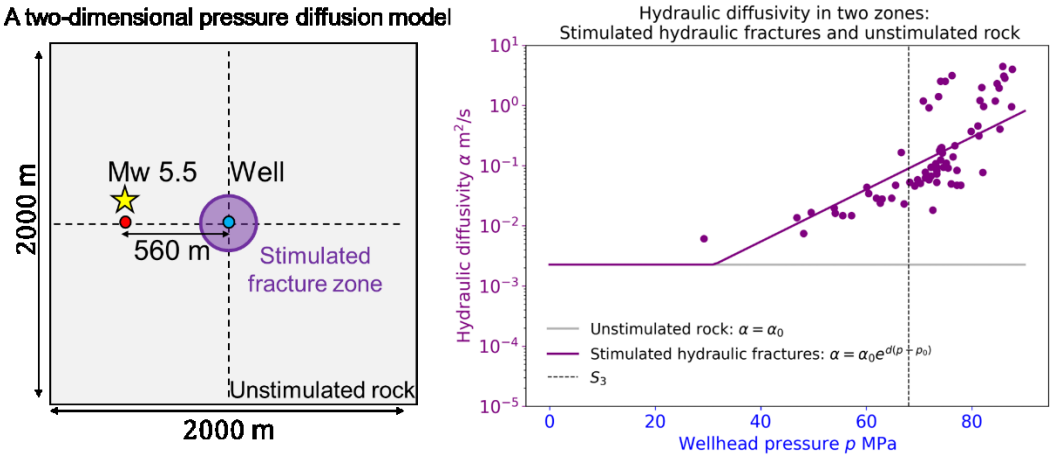

Figure 4: Pressure-diffusion model geometry (left) and hydraulic diffusivity formulation (right).

3.2.2 Hydraulic diffusivity formulation

Hydraulic diffusivity is prescribed differently for the two zones in Figure 4. In the unstimulated basement, diffusivity is assumed to keep constant in Equation (2):

$$\alpha = \alpha_0 \tag{2}$$

where α_0 is the diffusivity of unstimulated basement rock (0.0023 m^2/s) (Chang et al., 2020).

Within the stimulated hydraulic-fracture zone, diffusivity varies with pressure according to an exponential relation (Rutqvist et al. 1998, 2003) in Equation (3):

$$\alpha(p) = \alpha_0 e^{d(p-p_0)} \tag{3}$$

where d is the enhancement coefficient (0.05 MPa-1) and p_0 is the threshold pressure above which diffusivity becomes pressure dependent (31 MPa). This formulation is calibrated from in-situ injectivity test data from the Pohang site (Park et al., 2017; Park et al., 2020; Yeo et al., 2020) and captures the strong diffusivity enhancement during injection and the sharp collapse during depressurization.

3.2.3 Wellhead pressure boundary condition: rapid flowback reference case

Wellhead pressure $p_{\text{well}}(t)$is prescribed to represent injection and flowback operations. During injection, well pressure is fixed at the maximum wellhead pressure $\bar{p}_{\text{inj}} = 90$MPa for 17 days (Park et al., 2017, 2020). To represent the mitigation strategy implemented at Pohang, rapid flowback is modeled by abruptly reducing wellhead pressure to zero immediately after injection stops described in Equation (4):

$$\begin{cases} p_{well} = \bar{p}_{inj}, 0 < t \le t_{inj} \\ p_{well} = 0, t > t_{inj} \end{cases} \tag{4}$$

The total simulation period spans 75 days (17 days injection + 58 days post-injection). This reference case directly tests the hypothesis of Section 3.1 under the operational conditions preceding the Mw 5.5 earthquake and provides a baseline for evaluating mitigation performance.

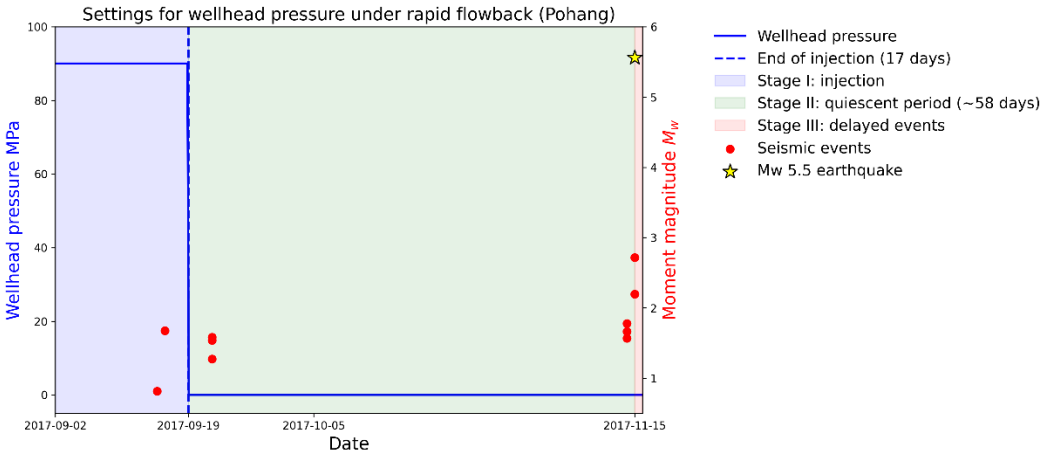

Figure 5: Prescribed wellhead pressure history for the rapid flowback reference case (Pohang scenario).

3.3 Mitigation strategies accounting for pressure-sensitive stimulated fractures

Building on the Pohang reference case, we investigated mitigation strategies aimed at improving pressure reduction accounting for pressure-dependent fracture behavior. Two directions were investigated: modifying well operation strategies and modifying stimulated fracture hydraulic properties.

3.3.1 Well operation strategies: shut-in, gradual flowback and rapid flowback

The first approach focuses on controlling the rate of wellhead pressure reduction during post-injection mitigation. Rapid pressure reduction maximizes the reverse pressure gradient toward the well but also promotes rapid fracture closure and diffusivity collapse. Because flowback rate is proportional to the product of hydraulic diffusivity and pressure gradient (Darcy's law), this trade-off may limit net fluid withdrawal from regions further from the well. We therefore evaluate three post-injection strategies (Figure 6): (1) **Shut-in**, in which no fluid is allowed to be injected and withdrawn and pressure dissipates solely by diffusion into the reservoir with where wellhead pressure solved in Equation (5); (2) **Rapid flowback**, in which wellhead pressure is abruptly reduced to zero with wellhead pressure prescribed in Equation (6); and (3) **Gradual flowback**, in which wellhead pressure is reduced progressively, maintaining higher near-well pressure and diffusivity during early depressurization with wellhead pressure prescribed in Equation (7). These scenarios allow assessment of whether slower pressure reduction can enhance sustained flowback by preserving fracture hydraulic diffusivity.

$$q_{well}^{Shut-in}(t > t_{inj}) = 0 \rightarrow \frac{\partial p}{\partial x(x=x_{well})} = 0 \rightarrow p_{well}^{Shut-in}(t > t_{inj}) \tag{5}$$

$$p_{well}^{Rapid\ flowback}(t > t_{inj}) = 0 \tag{6}$$

$$p_{well}^{Gradual\ flowback}(t > t_{inj}) = p_{well}^{Shut-in} - 35MPa \tag{7}$$

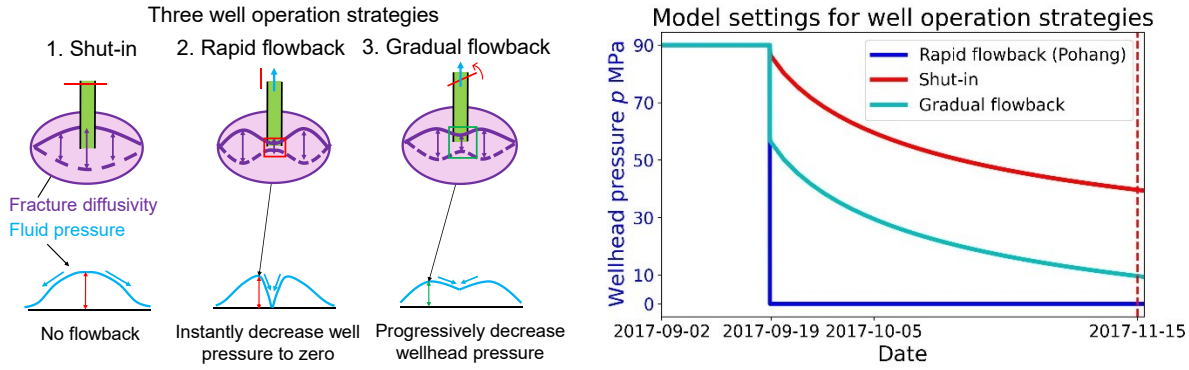

Figure 6: Well operation strategies (left) and corresponding model settings on wellhead pressure histories (right).

3.3.2 Modification of fracture hydraulic properties: Role of proppant

The second approach targeted fracture properties directly by weakening the coupling between diffusivity and pressure during depressurization. Proppants are small, stiff granular materials (e.g. sand) originally developed for hydraulic fracturing and increasingly adopted in recent EGS projects (e.g., Utah FORGE and Fervo). Proppants can mechanically support fracture apertures and limit closure as pressure decreases. At Pohang case, no proppant was used, and the fracture hydraulic diffusivity could greatly decrease during flowback. To evaluate the potential benefit of proppants on mitigation performance, we simulate an idealized case (Figure 7) in which stimulated fractures retain the maximum diffusivity achieved during injection throughout post-injection depressurization in Equation (8) and (9). This scenario represents the upper bound of proppant effectiveness. Combining the three well operation strategies with the presence or absence of proppant yields six mitigation scenarios, we evaluated early- and late-time reservoir pressure reduction and track pressure buildup at the Mw 5.5 location as an indicator of delayed seismicity on fault.

$$\alpha_{max}^{inj}(\boldsymbol{x}) = max\ \alpha\left(\boldsymbol{x}, t \le t_{inj}\right) = \alpha_0 e^{d(max\ p(\boldsymbol{x}, t \le t_{inj}) - p_0)} \tag{8}$$

$$\alpha_{prop}(\boldsymbol{x}, t) = \begin{cases} \alpha_0 e^{d(p(\boldsymbol{x},t) - p_0)}, t \le t_{inj} \\ \alpha_{max}^{inj}(\boldsymbol{x}), t > t_{inj} \end{cases} \tag{9}$$

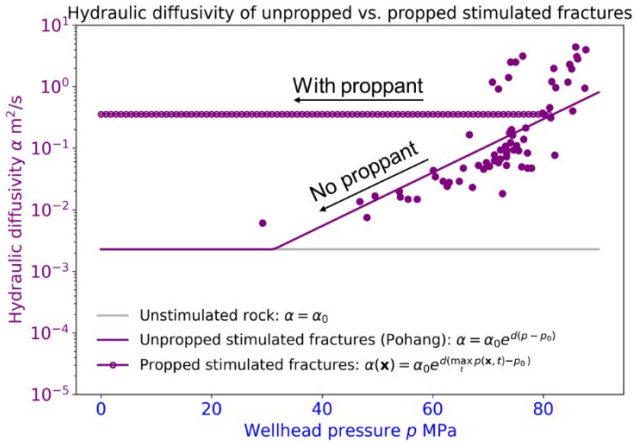

Figure 7: Hydraulic diffusivity formulation for propped fractures.

4. RESULTS

Before examining post-injection mitigation performance, we first summarize the modeled pressure and hydraulic diffusivity distribution at the end of injection. Because all mitigation strategies were initiated after injection stops, the pressure and diffusivity fields at the end of injection are identical across all scenarios and provide a common reference for comparison with post-injection behavior under different mitigation treatments.

Figure 8 shows the spatial distributions of fluid pressure and hydraulic diffusivity at the end of injection ($t_1 = t_{\mathrm{inj}}$). At this time, pressure near the PX-2 well ($x = 0$) reached approximately 90 MPa, consistent with the prescribed injection pressure. The region in which pressure exceeded the minimum principal stress ($S_3 = 68$ MPa) extended to approximately 160 m from the well, defining the stimulated hydraulic fracture zone. Within this stimulated zone, hydraulic diffusivity was strongly enhanced by fracture opening, reaching values of approximately 0.8 m²/s, nearly 350 times larger than the background basement diffusivity (0.0023 m²/s). Outside the stimulated zone,

diffusivity remained low and pressure-independent, reflecting intact basement conditions. At the end of injection, the pressure front had propagated to approximately 350 m from the well but had not yet reached the Mw 5.5 hypocenter located ~560 m away. This pressurization state provided a baseline for evaluating how pressure and diffusivity evolve during post-injection depressurization under different mitigation strategies.

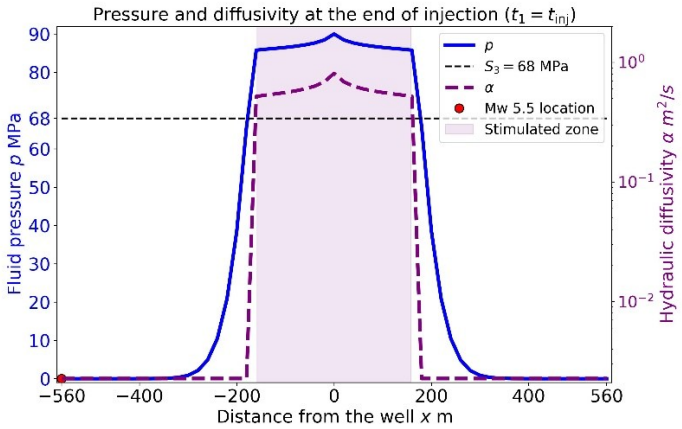

Figure 8: Pressure and hydraulic diffusivity distributions at the end of injection ($t_1 = t_{inj}$).

4.1 Baseline case: rapid flowback in unpropped fractures (Pohang scenario)

We first examined the reference scenario corresponding to the mitigation strategy implemented at Pohang, in which fractures are unpropped and rapid flowback is initiated immediately after injection stops. Figure 9 shows the spatial distributions of pressure and hydraulic diffusivity during the early post-injection period ($t_2 = t_{inj} + 16$ days) and at the time of the delayed Mw 5.5 earthquake ($t_3 = t_{inj} + 58$ days). Shortly after rapid flowback began, the well was opened to the atmosphere and wellhead pressure dropped abruptly to zero, generating a large reverse pressure gradient toward the well that, in principle, should promote efficient fluid withdrawal. However, this rapid depressurization near the well reduced pressure well below the minimum principal stress, causing stimulated fractures to close. As a result, hydraulic diffusivity within the near-well fracture zone collapsed sharply.

As shown in Figure 9 (left), the region that previously acted as a high-diffusivity conduit during injection transitions into a low-diffusivity zone that impedes flow from regions farther from the well. Consequently, pressure reduction was largely confined to the vicinity of the well, while elevated pressure remained trapped in the reservoir outside the near-well zone, reaching values of ~50 MPa during the early post-injection period. Because pressure diffusion through the low-diffusivity basement is slow, this trapped pressure decayed only gradually. By the late post-injection period (Figure 9, right), elevated reservoir pressure remained substantial (~30 MPa) despite nearly two months of flowback. At this time, the pressure front had reached the fault, initiating pressure buildup at the Mw 5.5 hypocenter, where pressure increased to approximately 0.54 MPa.

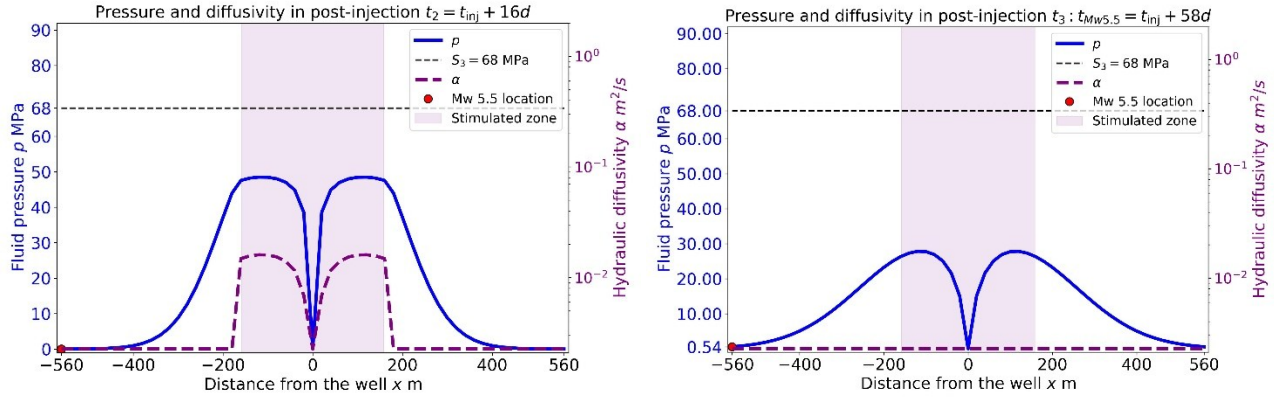

Figure 9: Pressure and hydraulic diffusivity distributions during rapid flowback in unpropped fractures in early-postinjection (t_2=t_{inj}+16d, left), and late post-injection at the time of the Mw 5.5 event (t_3=t_{inj}+58d, right)

The resulting fault pressure evolution is shown in Figure 10. Following injection termination, fault pressure increased monotonically due to pressure diffusion driven by the large trapped reservoir pressure. Approximately 58 days after injection stops, fault pressure reached ~0.54 MPa, sufficient to activate the fault and potentially trigger delayed seismicity. These results directly supported the hypothesis proposed in Section 3.1: when hydraulic diffusivity in stimulated fractures is strongly pressure-dependent, rapid flowback may be

ineffective at reducing overall reservoir pressure. Although rapid flowback produces a large pressure drop near the well, the associated collapse in diffusivity blocks sustained flowback from regions farther away, allowing large excess pressure to persist and drive delayed fault pressurization.

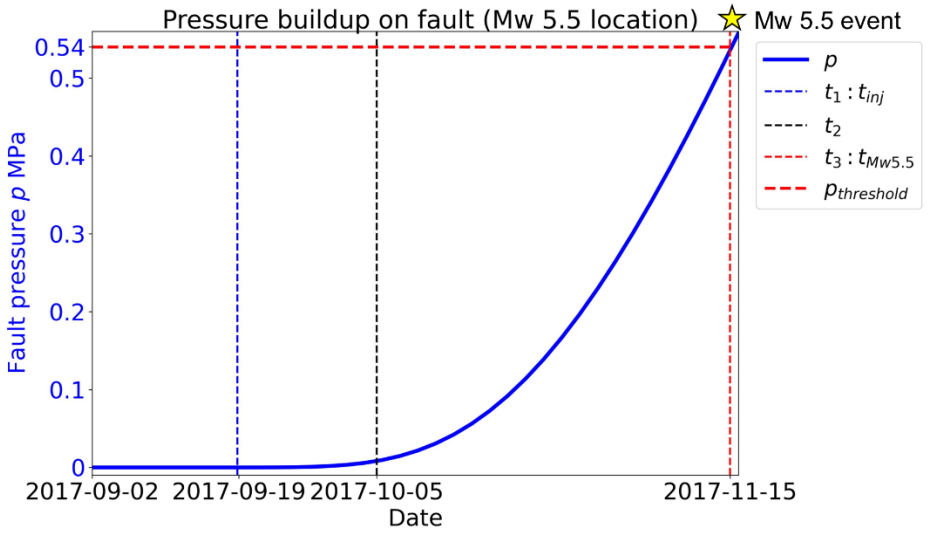

Figure 10: Pressure buildup at the Mw 5.5 location under rapid flowback in unpropped fractures (Pohang scenario)

4.2 Limited effectiveness of well operation strategies in unpropped fractures

The baseline Pohang scenario indicates that rapid flowback may not be the most effective mitigation strategy when the fracture hydraulic diffusivity is strongly pressure-dependent. To further assess the role of well operation strategies, we compared rapid flowback with shut-in and gradual flowback under unpropped fracture conditions representative of the Pohang site. Figure 11 shows pressure and hydraulic diffusivity distributions during the early post-injection period ($t_2 = t_{\text{inj}} + 16$ days) for the three well operation strategies. Under shut-in, no fluid was withdrawn, and pressure decreased solely through diffusion, resulting in the highest pressure throughout the reservoir. Under rapid flowback, pressure near the well dropped most rapidly, but near-well diffusivity collapsed sharply, limiting pressure reduction at larger distances. A crossover distance was observed in Figure 11 (left), beyond which pressure under gradual flowback becomes lower than under rapid flowback. This behavior suggested that although gradual flowback maintains higher near-well pressure and diffusivity, it enables more sustained pressure reduction in regions farther from the well particularly relevant for the distant Mw 5.5 fault location.

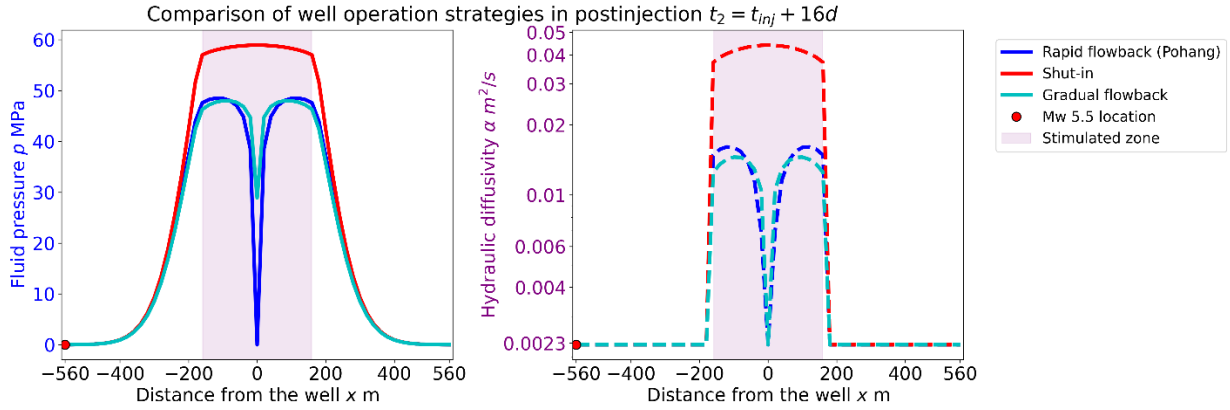

Figure 11: Pressure (left) and hydraulic diffusivity (right) distributions during early post-injection under shut-in, rapid flowback, and gradual flowback in unpropped fractures.

Figure 12 compares fault pressure buildup for the three strategies. Immediate shut-in performed worst, producing the fastest and largest fault pressurization. Among the flowback strategies, rapid flowback resulted in faster fault pressure buildup than gradual flowback. This indicates that immediately opening the well can be counterproductive when diffusivity is pressure-sensitive, as the rapid loss of diffusivity outweighs the benefit of a large reverse pressure gradient. Although gradual flowback modestly delayed fault pressurization relative to rapid flowback, all three strategies ultimately allowed fault pressure to approach activation threshold values. These results demonstrate that modifying well operation strategies alone provides only limited mitigation benefit under unpropped, pressure-sensitive fracture conditions.

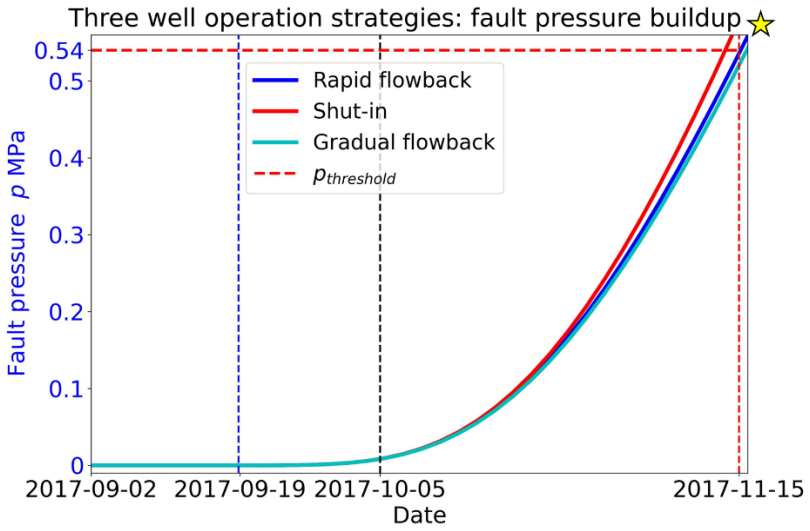

Figure 12: Pressure buildup at the Mw 5.5 fault location under three well operation strategies in unpropped fractures.

4.3 Effect of proppant under rapid flowback

We next examined the effect of modifying fracture hydraulic properties by introducing proppant, which preserves fracture aperture and diffusivity during depressurization and weakens the strong pressure dependence observed in unpropped fractures. Figure 13 compares pressure and hydraulic diffusivity distributions between unpropped and propped fractures under rapid flowback during early and late post-injection periods. When fractures are propped, hydraulic diffusivity within the stimulated zone remains high during depressurization instead of collapsing near the well. As a result, pressure reduction is effective not only near the well but also throughout the reservoir. Under otherwise identical rapid flowback conditions, peak trapped reservoir pressure during the early post-injection period decreased from ~50 MPa in the unpropped case to ~10 MPa in the propped case. By the time of the Mw 5.5 event, trapped pressure decreased further from ~30 MPa (unpropped) to ~2 MPa (propped). These results show that preserving high fracture diffusivity during depressurization dramatically reduces trapped reservoir pressure.

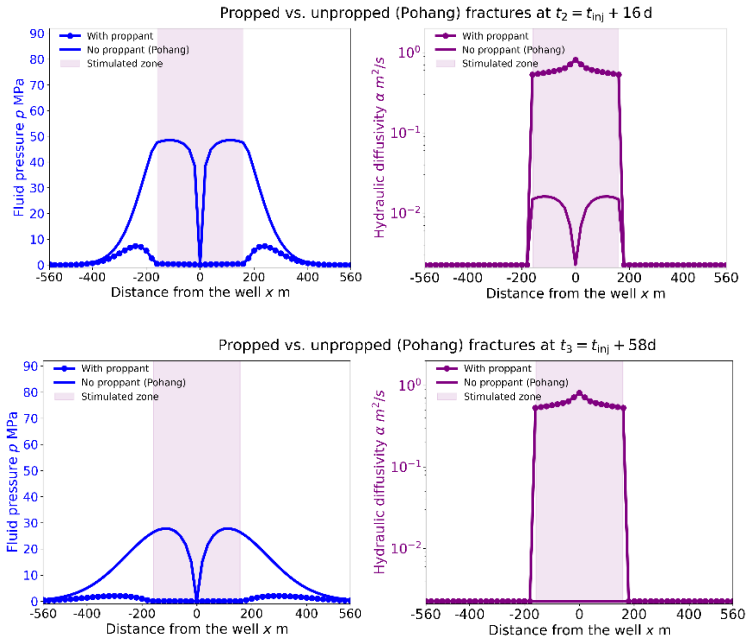

Figure 13: Comparison of pressure and hydraulic diffusivity distributions between unpropped and propped fractures under rapid flowback during early and late post-injection periods.

Figure 14 shows the corresponding fault pressure evolution. In the unpropped case, fault pressure increased steadily and reached ~0.54 MPa by ~60 days. In contrast, with propped fractures, fault pressure increased much more slowly and remains well below the activation

threshold throughout the simulation. These results indicate that rapid flowback combined with proppant can substantially reduce delayed fault pressurization and may effectively mitigate delayed seismicity.

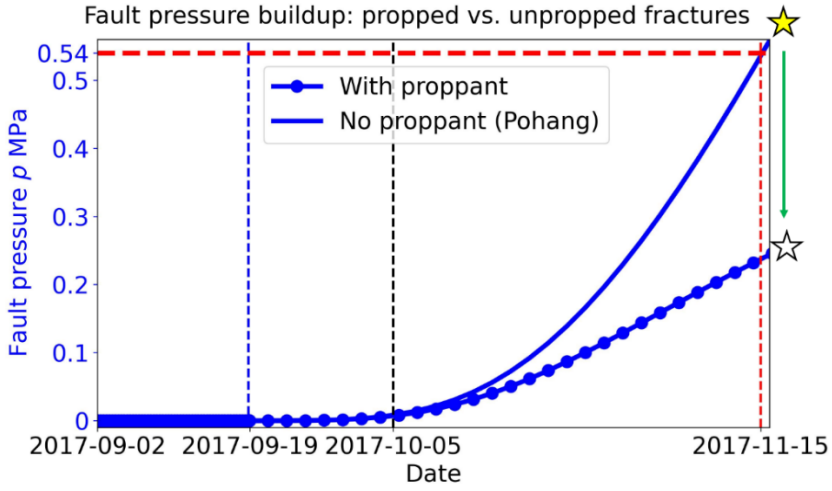

Figure 14: Fault pressure evolution for rapid flowback in unpropped and propped fracture cases.

4.4 Performance of well operation strategies in propped fractures

We next compared the effectiveness of different well operation strategies in the presence of proppant. Figure 15 (left) shows pressure distributions under shut-in, gradual flowback, and rapid flowback during the early post-injection period, with the corresponding fault pressure evolution shown in Figure 15 (right). As in the unpropped case, immediate shut-in resulted in the highest reservoir pressure because no fluid is extracted. However, in contrast to unpropped fractures, rapid flowback now produced the largest pressure reduction both near the well and at larger distances, because high diffusivity was preserved by proppant support. Gradual flowback yielded intermediate pressure reduction. Consequently, fault pressure buildup was the slowest under rapid flowback, followed by gradual flowback, with shut-in again performing worst. These results indicate that when fracture diffusivity is preserved during depressurization, rapid flowback becomes the most effective mitigation strategy.

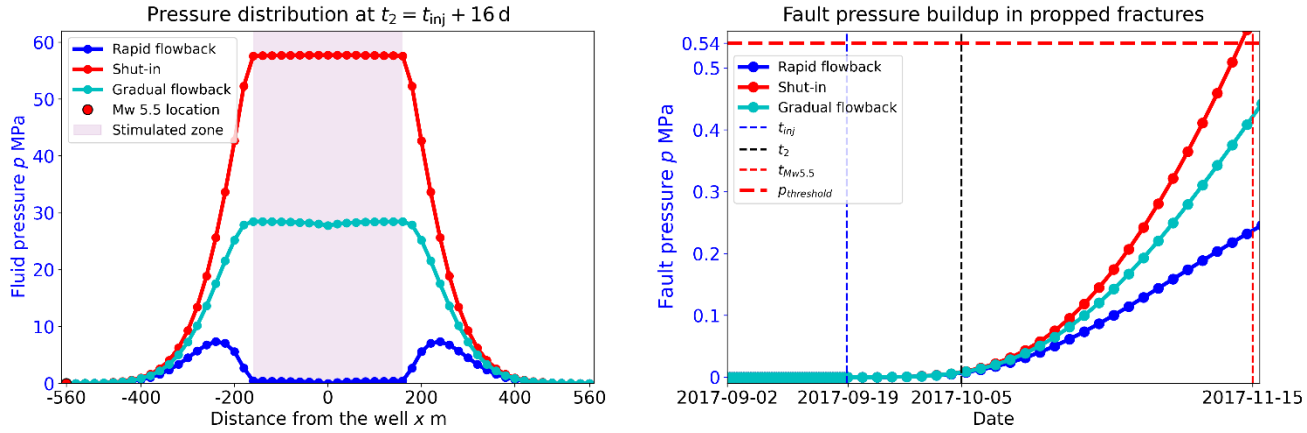

Figure 15: Pressure and hydraulic diffusivity distributions (left) and corresponding fault pressure evolution (right) under three well operation strategies in propped fractures.

4.5 Summary and comparison of six mitigation strategies

Figure 16 summarizes fault pressure buildup for all six mitigation strategies combining three well operation strategies with the presence or absence of proppant. Immediate shut-in consistently performed worst regardless of fracture condition. In unpropped fractures, gradual flowback performed better than rapid flowback for reducing delayed fault pressurization, but the improvement was limited. In contrast, adding proppant produced a much larger reduction in fault pressure than any change in well operation strategy alone. The most effective mitigation strategy among all cases tested in this work is rapid flowback combined with proppant, which minimizes trapped reservoir pressure and results in the slowest and lowest fault pressure buildup. These results demonstrate that modifying fracture hydraulic properties has a substantially greater impact on post-injection pressure reduction and delayed seismicity risk than adjusting well operation strategies alone.

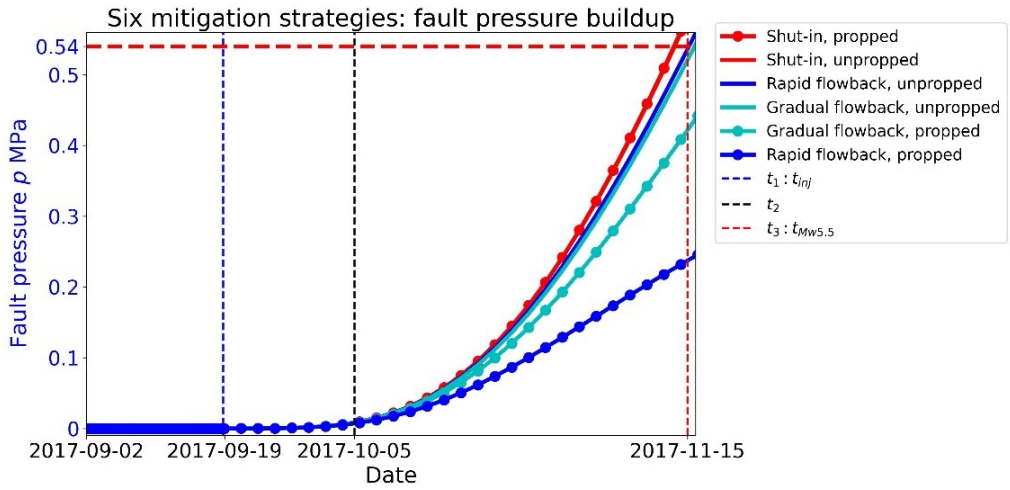

Figure 16: Comparison of fault pressure buildup for six mitigation strategies combining well operation and fracture condition.

5. DISCUSSION

5.1 Delayed seismicity at Pohang and pressure diffusion as a dominant mechanism

Previous studies of the Pohang EGS project have consistently identified fluid-pressure diffusion as the dominant mechanism responsible for the delayed Mw 5.5 earthquake (Ellsworth et al., 2019; Lim et al., 2019; Yeo et al., 2019; Chang et al., 2020). In these interpretations, elevated pore pressure generated during hydraulic stimulation continued to migrate outward after injection stopped, eventually reaching the fault, bringing up sufficient fault pressure increase, which reduces effective normal stress and triggers delayed seismic events. Because pressure diffusion beyond the stimulated fracture zone occurs primarily through low-diffusivity basement rock, the pressure front migration speed is slow, producing delays of up to months between injection termination and fault pressurization. This framework successfully explains the delayed timing of the Pohang earthquake.

However, while pressure diffusion provides a robust explanation for when the delayed earthquake occurred, it does not fully explain why the post-injection flowback mitigation strategy failed to substantially depressurize the reservoir. At Pohang, nearly two months of flowback recovered less than half of the injected fluid, indicating that pressure reduction remained limited despite sustained mitigation efforts. Most previous modeling studies have implicitly assumed constant hydraulic diffusivity along the flow path between the well and the fault. In contrast, in-situ injectivity tests at Pohang suggest that hydraulic diffusivity within the stimulated fracture zone near the well is strongly pressure-dependent and varies by up to three orders of magnitude during pressurization and depressurization. This discrepancy suggests that the hydraulic behavior of stimulated fractures during injection and post-injection mitigation may differ fundamentally, and that pressure-dependent fracture properties may exert a first-order control on flowback effectiveness which has not been explicitly examined in previous studies.

5.2 Mechanism of flowback failure: pressure-sensitive stimulated fractures

Motivated by this gap, we focus on the role of pressure-sensitive stimulated fractures in controlling flowback efficiency and reservoir depressurization during the post-injection period. To test this mechanism, we explicitly incorporate pressure-dependent hydraulic diffusivity into a pressure-diffusion model and evaluate the performance of multiple mitigation strategies. Our reference simulation represents the Pohang scenario with rapid flowback in unpropped fractures. The modelling results suggest that rapid depressurization near the well can be counterproductive when fracture diffusivity is strongly pressure-dependent. Although rapid flowback by abruptly decreasing wellhead pressure generates a large reverse pressure gradient toward the well, it simultaneously induces fracture closure and a sharp collapse in near-well diffusivity. As a result, the stimulated fracture zone transits from a flow-contributing conduit during injection to a low-diffusivity hydraulic barrier during depressurization. This diffusivity collapse hinders sustained flowback from regions further from the well, allowing high-magnitude excess pressure to remain trapped in the reservoir and continue diffusing toward the fault. Once the pressure front reaches the fault, this trapped pressure drives rapid fault pressurization, ultimately triggering delayed seismicity.

Exploring alternative well operation strategies shows that modifying the rate of wellhead depressurization alone provides only modest improvements. Gradual flowback preserves higher near-well diffusivity for longer times and can slow fault pressurization relative to rapid flowback for distant faults, but all unpropped scenarios ultimately allow fault pressure to approach activation thresholds. In contrast, modifying fracture hydraulic properties through proppant addition produces a substantially stronger effect. By maintaining high fracture diffusivity during depressurization, proppants enable effective pressure reduction throughout the reservoir. Among all tested strategies, rapid flowback combined with proppant yields the slowest and lowest fault pressure buildup. These results demonstrate that pressure-sensitive stimulated fractures can exert a critical influence on mitigation effectiveness in EGS and provide a physical explanation for the observed flowback failure at Pohang.

5.3 Practical considerations and alternative flowback configurations

The Pohang case involved stimulation of an open-hole well at a time when multistage hydraulic fracturing had not yet been widely adopted in EGS developments. This configuration simplified post-injection flowback operations. In contrast, several recent EGS projects employ multistage hydraulic fracturing in perforated wells, introducing additional operational constraints that directly affect mitigation strategy design. In perforated injection wells, rapid flowback can generate high flowback rates that mobilize proppant and lead to plugging of perforations or casing, potentially hindering subsequent stimulation stages. Mitigation strategies in such systems must therefore balance effective pressure reduction against the operational risks associated with flowback leading to proppant mobilization. One practical approach is gradual flowback, which maintains moderate flowback rates and can provide sufficient pressure reduction thereby slowing fault pressurization and reducing the likelihood of delayed seismic activation.

An alternative strategy is to conduct flowback from an offset well rather than from the injection well itself, particularly if the offset well is completed as an open-hole section intersecting the stimulated fractures generated by the injection well (Figure 15). This configuration can reduce operational risks at the perforated injection well while still enabling fluid withdrawal and enable effective pressure reduction from the reservoir. Our model results indicate that, in the absence of proppant, offset-well flowback provides only limited improvement: diffusivity collapse in the stimulated fractures hinders sustained fluid withdrawal, leading to high-magnitude trapped pressure that can rapidly load the fault once the pressure front arrives. In contrast, when fractures are propped and fracture hydraulic diffusivity is preserved during depressurization, both injection-well and offset-well flowback become effective. Under these conditions, rapid flowback from an open-hole offset well may offer the best compromise between mitigation effectiveness and constraints against mobilizing proppant, particularly for EGS developments applying multistage hydraulic fracturing.

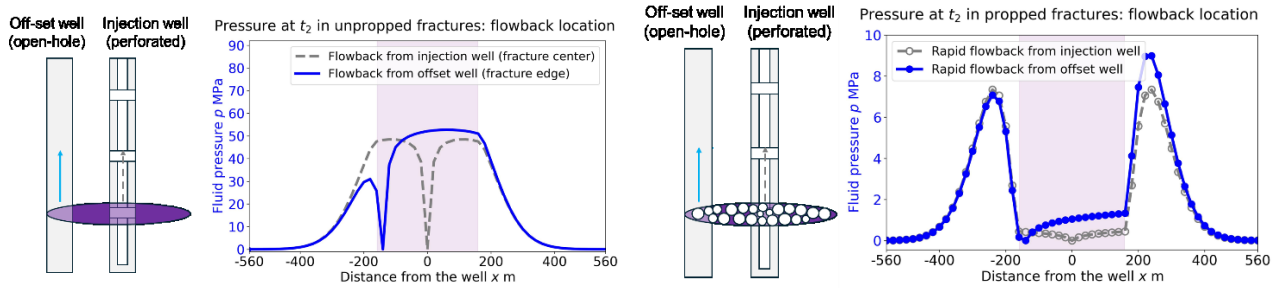

Figure 15: Pressure distribution in post-injection period ($t_2 = t_{inj} + 16d$) under different flowback configurations in unpropped fractures (left) and propped fractures (right)

5. CONCLUSION

This study investigated why prolonged post-injection flowback mitigation can fail to withdraw a substantial fraction of injected fluid and may not prevent delayed large-magnitude seismicity, focusing on the approximately two-month delayed Mw 5.5 earthquake at the Pohang Enhanced Geothermal System (EGS) site. Motivated by field observations indicating strongly pressure-dependent and largely reversible hydraulic diffusivity within the stimulated fracture zone around the well, we propose that pressure-sensitive stimulated fractures can play a key role in limiting flowback effectiveness and reservoir depressurization, thereby promoting delayed fault pressurization and increasing the risk of post-injection seismicity.

By constructing a pressure-diffusion model that explicitly incorporates pressure-dependent hydraulic diffusivity, we demonstrated that rapid flowback in unpropped fractures (the Pohang scenario) can be ineffective despite generating a large reverse pressure gradient toward the well. Rapid depressurization near the well induces closure of stimulated fractures and a sharp collapse in near-well hydraulic diffusivity, transforming the stimulated fracture zone from a high-transmissivity conduit into a low-diffusivity hydraulic barrier. This diffusivity collapse severely limits sustained flowback from regions further away from the well, allowing excess pore pressure of large magnitude to remain trapped in the reservoir for extended periods. The trapped pressure continues to diffuse toward the fault, ultimately producing substantial delayed fault pressurization. For the Pohang scenario, modeled fault pressure reached approximately 0.54 MPa at the Mw 5.5 hypocenter about two months after injection ceased, consistent with triggering of the delayed earthquake that was observed in the actual field.

We further demonstrated that modifying well operation strategies alone by changing the rate of wellhead depressurization provides only limited mitigation benefit when fracture diffusivity is strongly pressure-dependent and highly reversible. Although gradual flowback modestly slows and delays fault pressurization relative to rapid flowback, in the model all unpropped scenarios ultimately allow fault pressure to approach activation thresholds. In contrast, modifying fracture hydraulic properties to weaken the coupling between pressure and diffusivity by addition of proppant significantly changes post-injection pressure evolution. By preserving high fracture diffusivity during depressurization, proppants enable effective pressure reduction throughout the reservoir and substantially slow fault pressurization. Among all strategies tested, rapid flowback combined with proppant yielded the most effective mitigation, minimizing trapped reservoir pressure and maintaining fault pressure well below critical levels. These results highlight that post-injection seismic risk mitigation in EGS depends not only on operational control but critically on fracture hydromechanical behavior. Accounting for pressure-sensitive fracture properties is important for understanding mitigation failure and for designing more effective strategies to reduce seismic risk in post-injection.

REFERENCES

Alcolea, A., Meier, P., Vilarrasa, V., Olivella, S., and Carrera, J.: Hydromechanical Modeling of the Hydraulic Stimulations in Borehole PX-2 (Pohang, South Korea), Geothermics, 120, (2024), 103009.

Boyet, A.: Understanding and mitigating the post-injection seismicity induced by fluid injection in Enhanced Geothermal Systems, PhD thesis, Polytechnic University of Catalonia, (2023).

Boyet, A., de Simone, S., and Vilarrasa, V.: To bleed-off or not to bleed-off?, Geophysical Research Letters, 51(23), (2024a).

Boyet, A., Vilarrasa, V., Rutqvist, J., and de Simone, S.: Forecasting fluid-injection induced seismicity to choose the best injection strategy for safety and efficiency, Philosophical Transactions of the Royal Society A, 382(2276), (2024b).

Catalli, F., Rinaldi, A. P., Gischig, V., Nespoli, M., and Wiemer, S.: The importance of earthquake interactions for injection-induced seismicity: Retrospective modeling of the Basel Enhanced Geothermal System, Geophysical Research Letters, 43(10), (2016), 4992–4999.

Chang, K. W., Yoon, H., Kim, Y. H., and Lee, M. Y.: Operational and geological controls of coupled poroelastic stressing and pore-pressure accumulation along faults: induced earthquakes in Pohang, South Korea, Scientific Reports, 10, (2020).

Deichmann, N., and Giardini, D.: Earthquakes induced by the stimulation of an enhanced geothermal system below Basel (Switzerland), Seismological Research Letters, 80(5), (2009), 784–798.

Ellsworth, W. L.: Injection-induced earthquakes, Science, 341, (2013), 1225942.

Ellsworth, W. L., Giardini, D., Townend, J., Ge, S., and Shimamoto, T.: Triggering of the Pohang, Korea, earthquake (Mw 5.5) by enhanced geothermal system stimulation, Seismological Research Letters, 90(5), (2019), 1844–1858.

Häring, M. O., Schanz, U., Ladner, F., and Dyer, B. C.: Characterisation of the Basel 1 enhanced geothermal system, Geothermics, 37(5), (2008), 469–495.

Horne, R., Genter, A., McClure, Ji M., Ellsworth, W., Norbeck, J., and Schill, E.: Enhanced geothermal systems for clean firm energy generation, Nature Reviews Clean Technology, 1(2), (2025), 148–160.

Kivi, I. R., Boyet, A., Wu, H., Walter, L., Hanson-Hedgecock, S., Parisio, F., and Vilarrasa, V.: Global physics-based database of injection-induced seismicity, Earth System Science Data, 15(7), (2023), 3163–3182.

Kivi, I. R., Vilarrasa, V., Kim, K. I., Yoo, H., and Min, K. B.: Bleed-off control on post-injection seismicity in enhanced geothermal systems, Underground Space, 22, (2025), 21–38.

Lim, H., Deng, K., Kim, Y. H., Ree, J. H., Song, T. R. A., and Kim, K. H.: The 2017 Mw 5.5 Pohang earthquake, South Korea, and poroelastic stress changes associated with fluid injection, Journal of Geophysical Research: Solid Earth, 125(6), (2020).

Min, K. B., Park, S., Kim, K. I., Yoo, H., Kwon, S., Yim, J., and Rutqvist, J.: Enhancement of steam phase relative permeability due to phase transformation effects in porous media, Proceedings, 48th Workshop on Geothermal Reservoir Engineering, Stanford University, Stanford, CA (2023).

Moein, M. J. A., Langenbruch, C., Schultz, R., Grigoli, F., Ellsworth, W. L., Wang, R., Rinaldi, A. P., and Shapiro, S.: The physical mechanisms of induced earthquakes, Nature Reviews Earth & Environment, 4(12), (2023), 847–863.

Murphy, H., Huang, C., Dash, Z., Zyvoloski, G., and White, A.: Semianalytical solutions for fluid flow in rock joints with pressure-dependent openings, Water Resources Research, 40(12), (2004).

Rutqvist, J., and Stephansson, O.: The role of hydrochemical coupling in fractured rock engineering, Hydrogeology Journal, 11(1), (2003), 7–40.

Rutqvist, J., Noorishad, J., Tsang, C. F., and Stephansson, O.: Determination of fracture storativity in hard rocks using high-pressure injection testing, Water Resources Research, 34(10), (1998), 2551–2560.

Tangirala, S. K., Parisio, F., Vaezi, I., and Vilarrasa, V.: Effectiveness of injection protocols for hydraulic stimulation in enhanced geothermal systems, Geothermics, 120, (2024).

Witherspoon, P. A., Wang, J. S. Y., Iwai, K., and Gale, J. E.: Validity of cubic law for fluid flow in a deformable rock fracture, Water Resources Research, 16(6), (1980), 1016–1024.

Woo, J.-U., Kim, M., Sheen, D.-H., Kang, T.-S., Rhie, J., Grigoli, F., et al.: An in-depth seismological analysis revealing a causal link between the 2017 Mw 5.5 Pohang earthquake and EGS project, Journal of Geophysical Research: Solid Earth, 124, (2019), 13060–13078.

Yeo, I. W., Brown, M. R. M., Ge, S., and Lee, K. K.: Causal mechanism of injection-induced earthquakes through the Mw 5.5 Pohang earthquake case study, Nature Communications, 11, (2020).

Zheng, Z.: Hydraulic fractures of the dipole type subject to fluid withdrawal through a conduit, Journal of Fluid Mechanics, 1007, (2025a).

Zheng, Z.: The deflation of a hydraulic fracture subject to fluid withdrawal through a narrow conduit: the influence of material toughness, Journal of Fluid Mechanics, 1007, (2025b).